한국염색가공학회지
pISSN 1229-0033, eISSN 2234-036X
Research Paper
https://doi.org/10.5764/TCF.2018.30.2.63

Fluorescence-Quenched Sensor for Trinitophenol in Aqueous Solution Based on Sulfur Doped Graphitic Carbon Nitride

*Corresponding author
Young-A Son
(yason@cnu.ac.kr)

Kyeong Su Min, Ramalingam Manivannan, Angu Satheshkumar and Young-A Son*
Department of Advanced Organic Materials Engineering, Chungnam National University, Daejeon, Korea

Received_April 13, 2018
Revised_May 21, 2018
Accepted_June 18, 2018

Abstract In this study, we report on successful attempt towards the synthesis of sulfur self-doped g-C_3N_4 by directly heating thiourea in air. The synthesized materials were characterized using UV-vis spectral technique, FT-IR, XRD and TEM analysis. Further, the obtained material shows an excellent detection of carcinogenic TNP(Tri nitro phenol) in the presence of 10-fold excess of various other common interferences. The strong inner filter effect and molecular interactions(electrostatic, π-π, and hydrogen bonding interactions) between TNP and the S-g-C_3N_4 Nano sheets led to the fluorescence quenching of the S-g-C_3N_4 Nano sheets with an excellent selectivity and sensitivity towards TNP compared to that of other nitro aromatics under optimal conditions and the detection limit calculated was found to be 6.324 nM for TNP. The synthesized nanocomposite provides a promising platform for the development of sensors with improved reproducibility and stability for ultra-sensitive and selective sensing of TNP.

Keywords *sulfur, g-C_3N_4, fluorescence, sensing, trinitophenol*

Textile Coloration and Finishing
TCF 30-2/2018-6/63-69

1. Introduction

In recent years nitro aromatic compounds plays a vital role in the preparation of pesticides, pharmaceuticals, explosives, leather, dyes, military industries, chemical fibers, fireworks, matches and rubber products[1]. There are various nitro aromatic compounds used as an explosives are existing such as Trinitrophenol(TNP), Trinitrotoluol(TNT), Methyldinitrobenzene (DNT), Trimethylenetrinitramine(RDX), Nitrobenzol (NB), Dimethyl-dinitro-n-butane(DMNB), and Nitrocarbol(NM), among these TNP tend to have greater explosive nature when compared to that of TNT[2]. These compounds are major source for polluting groundwater as well as soils due to their explosivity and high toxicity[3,4]. TNP owes considerable attention, it is not only directly contaminating the environment but also causes a threat to human beings, leading to skin exasperation, causes damage to liver or kidney, different types of cyanosis and a rare type of aplastic anemia when inhaled, ingest or by touch[5,6]. Even the nitro aromatic compounds causing threat to the society but there are relatively less efforts has been paid to detect nitro aromatic explosives for the purpose of environmental safety and national security and cost performances of degradation[7,8]. Numerous methods were developed to detect these types of molecules, such as mass spectroscopy, photo fragmentation using laser, gas chromatography with electron capture and X-ray imaging. In addition, colorimetric detection[9] and fluorescence techniques were adopted for the detection[10]. Among these techniques, fluorescence sensing considered to be simple handling with high sensitivity short response time, and can be examined both in solution and solid phase, moreover it's a cost-effective process[11].

The graphitic carbon nitride(g-C_3N_4), a metal free n-type semiconductor polymer possesses properties

like exceptional electric, optical, physiochemical ability and have a lower production cost[12,13]. Which make g-C_3N_4 and its derivatives have been studied widely in various fields includes, bioimaging hydrogen devices, lithium ion storage, optoelectronic device and catalysts[14,15]. Additionally, g-C_3N_4 Nano sheets of atomic scale thickness and high specific surface area, it promotes photo/electro response. Many attempts have been implemented to improve the quantum efficiency, stability, safety and cheapness of g-C_3N_4, such as preparing mesoporous structure[16] and hollow Nano spheres[17], doping with nonmetal species such as sulfur an effective dopant and has the ability to narrow down the band gap[18,19]. In this study, the as-prepared samples exhibited potential application for selective and sensitive detection of 2, 4, 6-trinitrophenol (TNP) could provide new insights into the supported S-g-C_3N_4 composite materials for environmental pollution detection with public safety and security.

2. Experimental section

2.1 Synthesis and characterization of S-g-C_3N_4

The S-g-C_3N_4 was prepared more efficiently by a simple heating method. In which 6g of thiourea was taken in an alumina crucible with a lid, and it was heated gradually between the temperature ranges of 450~575 ˚C for 2h by increasing temperature at a rate of 2 ˚C min^{-1} in atmospheric air, followed by cooling to room temperature. The resultant yellow composite material was collected and ground into powders for use without further treatment. Scheme 1 shows the formation mechanism of the S-doped g-C_3N_4.

2.2 Characterization

The UV-Vis spectra was measured using UV-2400 spectrophotometer (Shimadzu, Japan) with barium sulfate as reference. FT-IR spectra were recorded using a Perkin Elmer Spectrum One spectrophotometer equipped with a diamond probe ATR attachment (neat sample). XRD analysis was carried out in an X-ray diffraction unit, Cu Kα radiation (λ = 1.5418° A) on X-pert pro MPD high performance X-ray diffractometer. The material morphology was identified by High-resolution transmission electron microscopy (HR-TEM) carried out on TEM, FEI TECNAI T20 G2. The sample preparation for TEM analysis carried out by placing a drop of solution on carbon-coated copper grid and dried Fluorescence spectra were recorded using a Varian Cary Eclipse fluorescence spectrophotometer (1 cm quartz cell) at 25℃.

2.3 Fluorescence sensing of TNP

A stock solution(50 μ L) of S-g-C_3N_4 Nano sheets was mixed with a 10 mM Tris- HCl buffer(pH 8.0) containing different concentrations(0 to 300 μ M) of TNP. The volume of solution kept constant 1.0 mL each concentration and kept the solution at room temper-

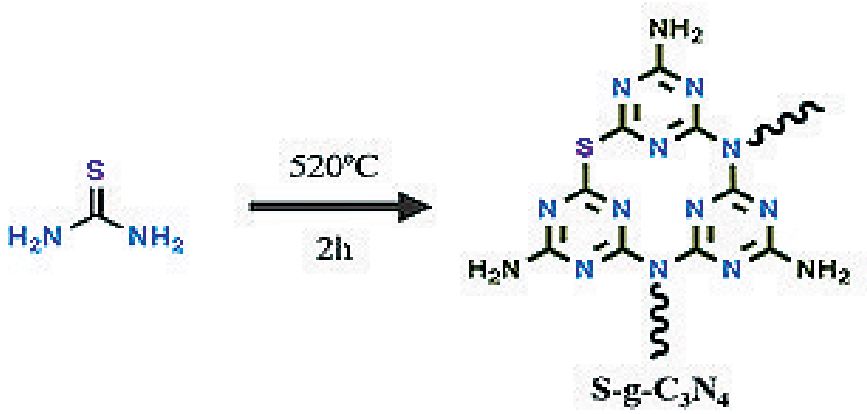

Scheme 1. The mechanism of the S-doped g-C_3N_4.

ature for 5 min and the fluorescence intensity of the solutions were measured between the wavelength range of 400nm to 590nm by exciting 310nm. Further the sensitivity for other nitro aromatics(TNT, DNT, RDX, NB, DMNB, and NM) with S-g-C_3N_4 was measured by adding above mentioned nitro aromatics at the same conditions and concentrations.

3. Results and discussion

3.1 UV-Vis absorption spectra

UV-Vis C_3N_4 Nano sheets were studied. A strong absorption peak at 350nm is attributed to the pure g-C_3N_4(Figure 1(curve a)) and after doping sulfur the absorption peak at 350nm is red shifted to 355nm (curve b), which is due to the doping of sulfur on to the surface of g-C_3N_4. The red-shift is due to the enhanced structural connections due to the improved Vander Waals interaction between the tri-s-triazine cores.

3.2 FT-IR

The functional composite material of S-g-C_3N_4 and g-C_3N_4 was confirmed by the FTIR spectroscopy(Figure 2).

The many small peaks observed in the range of 900-1800 cm^{-1} correspond to stretching vibrations of C=N, C-N, C-C or C-N-C bonds of C-N heterocycles[20,21]. One notable exception is the strong absorbance peak observed at 804 cm^{-1}, this peak has previously been attributed to the presence of s-triazine(g-C_3N_4). The band at 884 cm^{-1} is attributed to the out-of-plane bending vibration of characteristics of triazine rings[22].

Additionally, the broad band at 2900-3500 cm^{-1} corresponds to the stretching modes of N-H and C-H of g-C_3N_4[23]. Then above all the peaks which conforms the presence of g-C_3N_4 nanosheets[24,25]. Obviously, no peak was ascribed to the bond of sulfur with other elements because the amount of sulfur was too low[26].

3.3 XRD

To better understand the crystal structure, the as-prepared g-C_3N_4 and S-g-C_3N_4 was revealed by XRD. Figure 3(a) shows the XRD pattern of pristine g-C_3N_4 displays two distinct diffraction peaks located at 2 θ of about 13.1° and 27.3°, which are in good accordance with the characteristic peaks of g-C_3N_4. These peaks correspond to the (1 0 0) and (0 0 2) crystal planes of g-C_3N_4[27]. The main peaks of sulfur-doped g-C_3N_4 slightly shift to small angle direction, in addition, close observation shows that the reflection at 13.61° becomes more prominent for S-doped g-C_3N_4 which may originate from the bending of the graphitic layer due to the distortion of in plane nitride pores by S

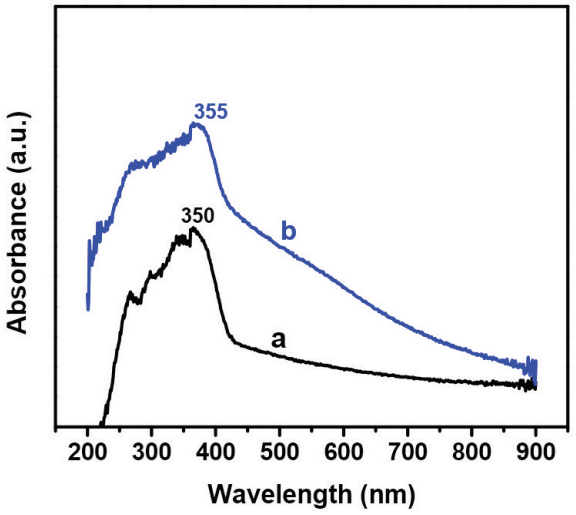

Figure 1. UV-Vis absorbance spectra of g-C_3N_4 (a) and S-g-C_3N_4 (b).

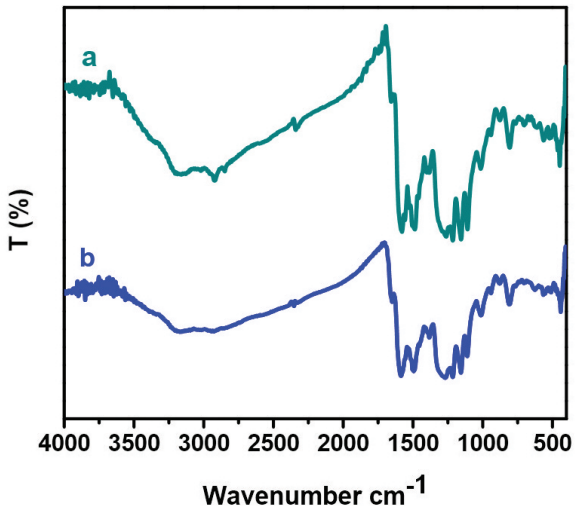

Figure 2. FT-IR spectra of g-C_3N_4 (a) and S-g-C_3N_4 (b).

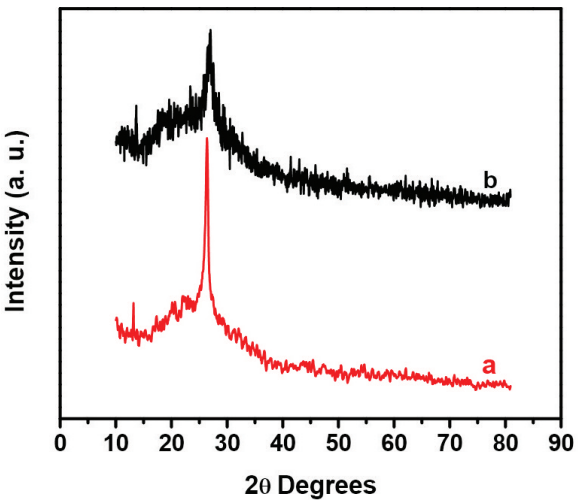

Figure 3. XRD patterns of g-C_3N_4(a) and S-g-C_3N_4(b).

doping as shown in Figure 3b.

This observation indicates that the crystal structure of S-doped g-C_3N_4 tends to become more stable[19]. These result good consistent with the literature report[28], from the XRD pattern, it was found that the crystallinity of S-doped g-C_3N_4 was 56.15% and the crystal size was found to be 3.26 nm using Scherer formula.

3.4 TEM

Figure 4A and Figure 4B displays the TEM images of surface and cross-section morphology of samples g-C_3N_4 and S-g-C_3N_4 respectively. It can be seen that the pure g-C_3N_4 sample consists of layer structure with several nanosheets as shown in Figure 4A. Thorough the observation of S-g-C_3N_4 Figure 4B revealed that the samples were grainy in structure, and their layered structures contain many irregular pores nature[29]. Moreover, compared with g-C_3N_4, the particles of S-g-C_3N_4 are thicker, which can be observed in Figure 4B.

3.5 Fluorescence determination of TNP

The sensing ability of S-g-C_3N_4 with the addition of increasing concentration of TNP was measured using fluorescence technique the spectra showed an emission maximum at 452 nm for S-g-C_3N_4 when excited at 310 nm and are shown in Figure 5. With an addition of increased concentration of TNP, the emission intensity of the peak at 452 nm was dramatically decreased by quenching the fluorescence of S-g-C_3N_4. Even with a very low concentration(1.0 nM TNP), the emission intensity of the sample S-g-C_3N_4 tend to show a noticeable change in the spectra. The observed change in intensity of the peak was mainly due to the interaction of TNP with S-g-C_3N_4 and also from the result it is noted that TNP sensing was more sensitive compared to that of other nitro aromatics. The quenching results could be quantitatively treated with the Stern-Volmer equation(1),

$$F^0/F = 1+K_{SV}[PA] \quad \cdots\cdots (1)$$

where,

F^0 and F : Represents the fluorescence intensity in

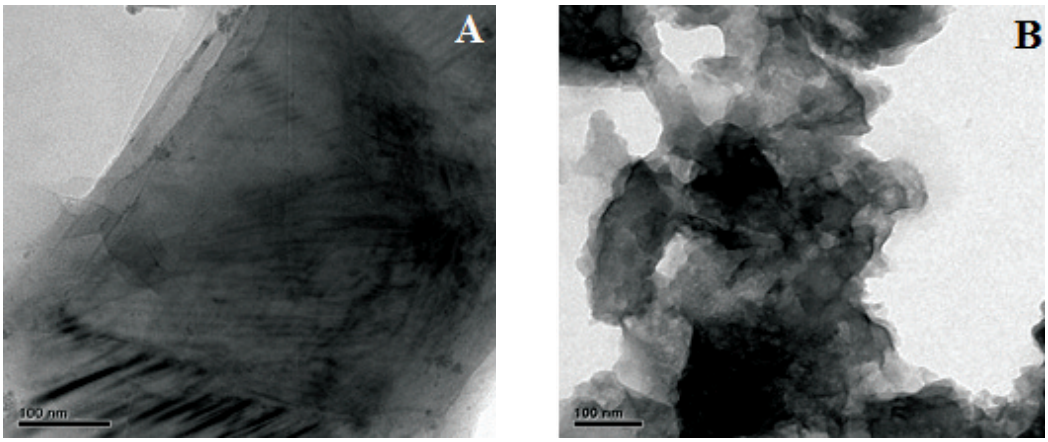

Figure 4. HR-TEM images of g-C_3N_4(A) and S-g-C_3N_4(B).

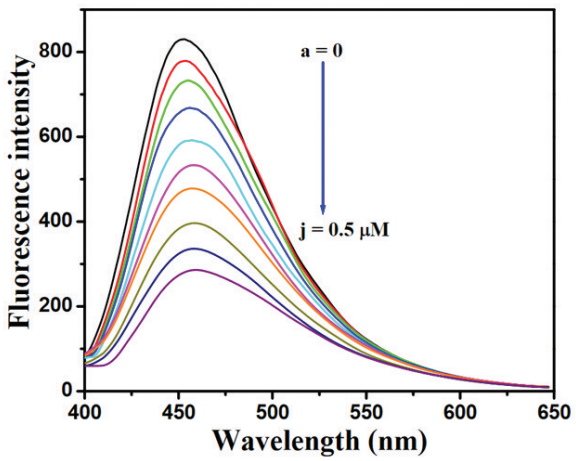

Figure 5. Fluorescence responses of the S-g-C_3N_4 nanosheets in the presence of different concentrations of TNP.

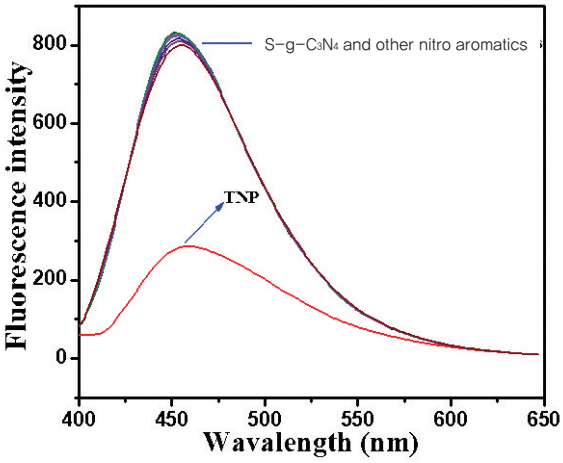

Figure 6. Fluorescence detection of S-g-C_3N_4 upon addition of various nitro aromatics such as TNP, TNT, DNT, RDX, NB, DMNB and NM.

presence and absence of TNP with S-g-C_3N_4

[PA] : Denotes the TNP concentration and Stern-Volmer constant(K_{SV}), with the fluorescence intensity and the concentration of TNP ranging from 1 nM to 0.5 μ M, the limit of detection (LOD) calculated was found to be 6.324 nM at a signal-to-noise ratio of 3.

From this experiments it is ascertained that the acidity, benzene and hydroxyl functionalities present in TNP has a possibility of interaction with the terminal amino group that is the basic site of triazine moiety on the g-C_3N_4 nanosheets and the interaction may be either electrostatic, π - π , or hydrogen bond formation. The most probable mechanism for this phenomenon is illustrated in Scheme 2.

3.6 Effect of interferences

The selectivity of the fluorescence characteristics of the g-C_3N_4 Nano sheets was evaluated by the addition of other nitro aromatics such as TNT, DNT, RDX, NB, DMNB, and NM in aqueous solution. The results indicated that the influence of other nitro aromatics was negligible and no noticeable change in fluorescence was observed. Whereas, with the addition TNP fluorescence peak intensity gets decreased significantly as shown in Figure 6.

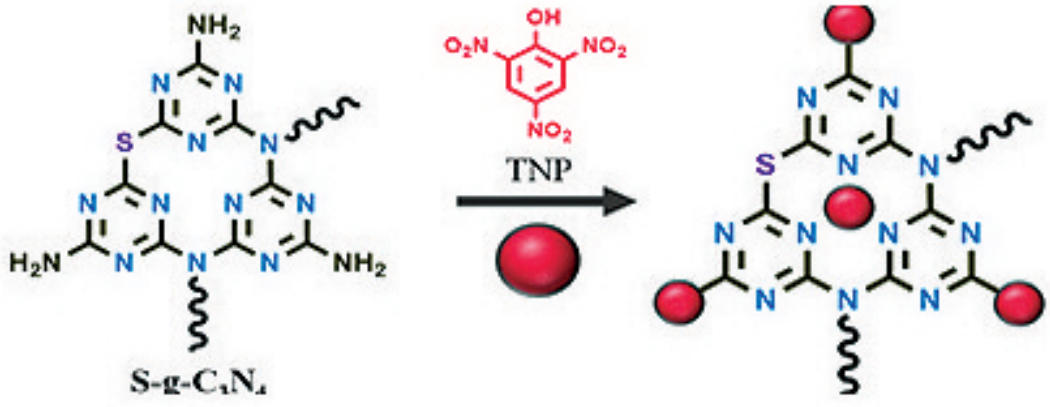

Scheme 2. The possible mechanism for the selective detection of TNP using S-g-C_3N_4.

4. Conclusions

In this study, we demonstrated an S-g-C_3N_4 Nano sheets, and its sensing ability towards TNP in a cost effective and simple fluorescence approach, the developed material showed high selectivity and sensitivity for TNP in aqueous solution, when compared to that of other nitro aromatic compounds. The limit of detection calculated was found to be 6.324nM for the determination of TNP solution. Even trace amounts of TNP in water samples can easily be identified using S-g-C_3N_4, and therefore the prepared material proves to be a potential probe for the detection of TNP.

Acknowledgments

This work was supported by research fund of Chungnam National University.

References

1. P. Kovacic and R. Somanathan, Nitroaromatic Compounds: Environmental Toxicity, Carcinogenicity, Mutagenicity, Therapy and Mechanism, *J. Appl. Toxicol*, **34**, 810(2014).
2. G. He, H. Peng, T. Liu, M. Yang, Y. Zhang, and Y. Fang, A Novel Picric Acid Film Sensor via Combination of the Surface Enrichment Effect of Chitosan Films and the Aggregation-induced Emission Effect of Siloles, *J. Mater. Chem.*, **19**, 7347(2009).
3. Y. Salinas, R. M. Manez, M. D. Marcos, F. Sancenon, A. M. Costero, M. Parra, and S. Gil, Optical Chemosensors and Reagents to Detect Explosives, *Chem. Soc. Rev.*, **41**, 1261(2012).
4. S. W. Thomas III, G. D. Joly, and T. M. Swager, Chemical Wensors based on Amplifying Fluorescent Conjugated Polymers, *Chem. Soc. Rev.*, **36**, 1339(2007).
5. J. Xiao, L. Qiu, F. Ke, Y. Yuan, G. Xu, Y. Wang, and X. Jiang, Rapid Synthesis of Nanoscaleterbium-based Metal-organic Frameworks by a Combined Ultrasound Vapour Phase Diffusion Method for Highly Selective Sensing of Picric Acid, *J. Mater. Chem. A*, **1**, 8745(2013).
6. J. F. Wyman, M. P. Serve, D. W. Hobson, L. H. Lee, and D. E. Uddin, Acute Toxicity, Dis-tribution, and Metabolism of 2,4,6-trinitrophenol(picric acid) in Fischer Rats, *J. Toxicol. Environ. Health*, **37**, 313(1992).
7. L. E. Kreno, K. Leong, O. K. Farha, M. Allendorf, R. P. V. Duyne, and J. T. Hupp, Metal-organic Framework Materials as Chemical Sensors, *Chem. Rev.*, **112**, 1105 (2012).
8. Y. Cui, Y. Yue, G. Qian, and B. Chen, Luminescent Functional Metal-organic Frameworks, *Chem. Rev.*, **112**, 1126(2012).
9. H. Lin and K. S. Suslick, A Colorimetric Sensor Array for Detection of Triacetone Triperoxide Vapor, *J. Am. Chem. Soc.*, **132**, 15519(2010).
10. D. Gao, Z. Wang, B. Liu, L. Ni, M. Wu, and Z. Zhang, Resonance Energy Transfer-amplifying Tluorescence Quenching at the Surface of Silica Nanoparticles toward Ultrasensitive Detection of TNT, *Anal. Chem.*, **80**, 8545(2008).
11. S. S. Nagarkar, B. Joarder, A. K. Chaudhari, S. Mukherjee, and S. K. Ghosh, Highly Selective Detection of Nitro Explosives by a Luminescent Metal-organic Framework, *Angew. Chem.*, **125**, 2953(2013).
12. X. Wang, K. Maeda, A. Thomas, K. Takanabe, G. Xin, J. M. Carlsson, K. Domen, and M. Antonietti, A Metal-free Polymeric Photocatalyst for Hydrogen Production from Water under Visible Light, *Nat. Mater.*, **8**, 76 (2009).
13. Y. Wang, X. Wang, and M. Antonietti, Polymeric Graphitic Carbon Nitride as a Heterogeneous Organocatalyst: from Photochemistry to Multipurpose Catalysis to Sustainable Chemistry, *Angew. Chem. Int. Edit.*, **51**, 68 (2012).
14. Y. Zhang, T. Mori, L. Niu, and J. Ye, Non-covalent Doping of Graphitic Carbon Nitride Polymer with Graphene: Controlled Electronic Structure and Enhanced Optoelectronic Conversion, *Energ. Environ. Sci.*, **4**, 4517(2011).
15. J. Zhu, Y. Wei, W. Chen, Z. Zhao, and A. Thomas, Graphitic Carbon Nitride as a Metal-free Catalyst for NO Decomposition, *Chem. Commun.*, **46**, 6965(2010).

16. F. Z. Su, S. C. Mathew, G. Lipner, X. Z. Fu, and M. Antonietti, mpg-C_3N_4-catalyzed Selective Oxidation of Alcohols using O_2 and Visible Light, *J. Am. Chem. Soc.*, **132**, 16299(2010).
17. J. H. Sun, J. S. Zhang, M. W. Zhang, M. Antonietti, X. Z. Fu, and X. C. Wang, Bioinspired Hollow Semiconductor Nanospheres as Photosynthetic Nanoparticles, *Nat. Commun.*, **3**, 1139(2012).
18. L. L. Feng, Y. Zou, C. Li, S. Gao, L. J. Zhou, and Q. Sun, Nanoporous Sulfur-doped Graphitic Carbon Nitride Microrods: A Durable Catalyst for Visible-light-driven H2 Evolution, *Int. J. Hydro Energy*, **39**, 15373(2014).
19. L. Ge, C. Han, X. Xiao, L. Guo, and Y. Li, Enhanced Visible Light Photocatalytic Hydrogen Evolution of Sulfur-doped Polymeric g-C_3N_4 Photo Catalysts, *Mater. Res. Bull.*, **48**, 3919(2013).
20. C. Liu, H. Huang, X. Du, T. Zhang, N. Tian, Y. Guo, and Y. Zhang, In situ Co-crystallization for Fabrication of g-C_3N_4/Bi_5O_7I Heterojunction for Enhanced Visible-light Photo Catalysis, *J. Phys. Chem. C*, **119**, 17156 (2015).
21. H. J. Kong, D. H. Won, J. Kim, and S. I. Woo, Sulfur-doped g-C_3N_4/$BiVO_4$ Composite Photo Catalyst for Water Oxidation under Visible Light, *Chem. Mater.*, **28**, 1318(2016).
22. Y. P. Zhu, T. Z. Ren, and Z. Y. Yuan, Mesoporous Phosphorus-doped g-C_3N_4 Nanostructured Flowers with Superior Photocatalytic Hydrogen Evolution Performance, *ACS Appl. Mater. Interfaces.*, **7**, 16850(2015).
23. Y. Yang, Y. Guo, F. Liu, X. Yuan, Y. Guo, S. Zhang, W. Guo, and M. Huo, Preparation and Enhanced Visible-light Photocatalytic Activity of Silver Deposited Graphitic Carbon Nitride Plasmonic Photo Catalyst, *Appl. Catal. B*, **142-143**, 828(2013).
24. R. C. Dante, P. M. Ramos, A. C. Guimaraes, and J. M. Gil, Synthesis of Graphitic Carbon Nitride by Reaction of Melamine and Uric Acid, *Mater. Chem. Phys.*, **130**, 1094 (2011).
25. D. Foy, G. Demazeau, P. Florian, D. Massiot, C. Labrugere, and G. Goglio, Modulation of the Crystallinity of Hydrogenated Nitrogen-rich Graphitic Carbon Nitrides, *J. Solid State Chem.*, **182**, 165(2009).
26. K. Wanga, Q. Li, B. Liu, B. Cheng, W. Ho, and J. Yu, Sulfur-doped g-C_3N_4 with Enhanced Photocatalytic CO_2-reduction Performance, *App. Catal. B*, **176-177**, 44 (2015).
27. G. G. Zhang, J. S. Zhang, M. W. Zhang, and X. C. Wang, Polycondensation of Thiourea into Carbon Nitride Semiconductors as Visible Light Photocatalysts, *J. Mater. Chem.*, **22**, 8083(2012).
28. L. Ge, C. Han, X. Xiao, L. Guo, and Y. Li, Enhanced Visible Light Photocatalytic Hydrogen Evolution of Sulfur-doped Polymeric g-C_3N_4 Photocatalysts, *Mater. Res. Bull.*, **48**, 3919(2013).
29. J. Xu, Y. J. Wang, and Y. F. Zhu, Nanoporous Graphitic Carbon Nitride with Enhanced Photocatalytic Performance, *Langmuir*, **29**, 10566(2013).